

This is the peer reviewed version of the following article:

Liu, H., Lukić, I., Miladinović, M.R., Veljković, V.B., Zdujić, M., Zhu, X., Zhang, Y., Skala, D.U., 2018. Continuous biodiesel production under subcritical condition of methanol – Design of pilot plant and packed bed reactor with MnCO₃/Na-silicate catalyst. *Energy Conversion and Management* 168, 494–504.
<https://doi.org/10.1016/j.enconman.2018.05.028>



This work is licensed under a [Creative Commons Attribution Non Commercial No Derivatives 4.0](https://creativecommons.org/licenses/by-nc-nd/4.0/) license

1 **Continuous biodiesel production under subcritical condition of**
2 **methanol – Design of pilot plant and packed bed reactor with MnCO₃/Na-**
3 **silicate catalyst**

4
5 Hui Liu^{1,*}, Ivana Lukić², Marija R. Miladinović³, Vlada B. Veljković³, Miodrag
6 Zdujic^{4,**}, Xiaosun Zhu¹, Yanan Zhang¹, Dejan U. Skala²

7
8 ¹ State Key Laboratory of Biogeology and Environmental Geology and School of
9 Environmental Studies, China University of Geosciences, Wuhan 430074, PR China

10 ² University of Belgrade, Faculty of Technology and Metallurgy, Karnegijeva 4, 11000
11 Belgrade, Serbia

12 ³ University of Niš, Faculty of Technology, Bulevar oslobođenja 124, 16000 Leskovac,
13 Serbia

14 ⁴ Institute of Technical Sciences of the Serbian Academy of Sciences and Arts, Knez
15 Mihailova 35, 11000 Belgrade, Serbia

16
17
18
19
20
21 *Corresponding author; E-mail address: zliuhui@hotmail.com (H. Liu). ** Co-corresponding
22 author: E-mail address: miodrag.zdujic@itn.sanu.ac.rs (M. Zdujic).

24 **Abstract**

25 The continuous biodiesel production from soybean oil was carried out under the
26 subcritical condition of methanol with $\text{MnCO}_3/\text{Na-silicate}$ as a heterogeneous catalyst. The
27 transesterification rate was first investigated in a set of experiments performed in a batch
28 autoclave at 448 K using methanol-to-oil molar ratio of 18:1 and various catalyst loadings (5, 10
29 and 20 wt% based on the oil mass). The results from these experiments, as well as the
30 experimental data and the appropriate kinetic model recently reported in the literature were used
31 for designing a packed bed tubular reactor (PBTR), a main unit of the pilot plant with the
32 capacity of 100 liters of biodiesel per day. The pilot plant was constructed and tested under
33 various operating conditions. The first 11 h of the pilot-plant operation was realized in the
34 tubular reactor packed with inert glass beads (i.e. without the catalyst) in order to analyze the
35 effect of the non-catalyzed subcritical biodiesel (fatty acid methyl esters, FAME) production.
36 Then, glass beads were replaced with a mix of $\text{MnCO}_3/\text{Na-silicate}$ catalyst particles and glass
37 beads, and the catalytic biodiesel production was continuously run under the subcritical methanol
38 condition for 85 h. Two mass balance tests during the continuous pilot plant operation were
39 performed.

40

41 **Keywords:** Biodiesel; Subcritical methanolysis; Kinetic modeling; $\text{MnCO}_3/\text{Na-silicate}$
42 catalyst; Pilot-plant design.

43

44

45 1. Introduction

46 In the past several years, many researchers have made efforts to synthesize efficient
47 heterogeneous catalysts for biodiesel production in order to substitute the conventional
48 technology based on homogeneous catalysis, which is currently applied in many industrial
49 facilities. Numerous investigations have been undertaken in order to estimate the potential
50 catalytic activity of both naturally originated and synthesized materials. Among the
51 heterogeneous catalysts, the CaO-based catalysts are frequently studied [1][2][3][4][5] due to
52 their high activity and possibility to be obtained from inexpensive natural and waste materials
53 [6]. The other low-cost materials, like MnCO_3 , Na-silicate and $\text{MnCO}_3/\text{Na-silicate}$, also show,
54 after thermal activation, a high catalytic activity for biodiesel production [7][8][9][10]. Some of
55 them, like Na-silicate, can be used even for transesterification of waste vegetable oils with a high
56 amount of water owing to the hydrolysis of the activated Na-silicate into OH^- and Si-O-H^+ , thus
57 avoiding soap formation. Another advantage is the simple regeneration of the used Na-silicate
58 catalyst with NaOH [7]. Other materials, like ion-exchange resins [11][12] and hydrotalcite [13],
59 have also been tested in order to obtain long-lifetime catalysts that can be used for continuous
60 processes.

61 Heterogeneously-catalyzed methanolysis reactions are slower than homogeneously-
62 catalyzed ones due to the mass transfer limitations in the three-phase system mainly at the
63 beginning of the transesterification process [14][15][16]. The nature of heterogeneously catalyzed
64 oil methanolysis reactions has been explained by different reaction mechanisms
65 [17][18][19][20][21][22]. However, the resulting kinetic models based on these mechanisms are
66 rather complex since a large number of parameters need to be determined. The recently reported
67 studies described the suitable, relatively simple kinetic models of the vegetable oil methanolysis
68 requiring no complicated computations [2][14]. The model proposed by Lukić et al. [14] is based
69 on the pseudo-first order kinetics that involves the triacylglycerols (TAGs) mass transfer and
70 chemical reaction controlled regimes. The model proposed by Miladinović et al. [2] includes a
71 changing reaction mechanism with respect to TAGs and the first order reaction with respect to
72 fatty acid methyl esters (FAMES). The applicability of both models was confirmed for the
73 sunflower oil methanolysis catalyzed by the CaO-based catalysts ($\text{CaO}\cdot\text{ZnO}$, pure CaO and

74 quicklime) under various reaction conditions [23][24]. They were applied and verified under
75 continuous conditions at small scale, too [13][23].

76 The continuous methanolysis has been investigated at both atmospheric pressure and
77 moderate temperature [11][21][25][26][27][28] and high pressure and temperature [29][30][31]
78 [32][33]. However, the most of the reported studies were conducted in laboratory scale devices
79 for a short period of time [34]. Kouzu et al. reported the pilot scale transesterification of the
80 waste cooking oil in the higher volume reactor (150 L), but it was performed in a stirred tank
81 reactor with powdery CaO catalyst since it was concluded that the CaO-catalyzed
82 transesterification is difficult to perform with the fixed bed reactor, due to the mass transfer
83 limitations as well as plausible crushing of catalysts particles [35]. Catalysts used in powder
84 form in the packed bed reactors caused blocking of the flow of the reactants throughout the
85 catalyst bed by particle agglomeration [28] and high pressure drop inside small column at the
86 end of the experiment due to the very dense packed bed formed [8]. Also, separation of the solid
87 catalyst in powder form from the products of transesterification is difficult, thus, important issue
88 for packed bed reactors, which are commonly used for continuous heterogeneously catalyzed
89 processes at the industrial scale, is the use of coarse catalyst particles, with good mechanical
90 strength that would not collapse during the process.

91 The recent investigations of the heterogeneously catalyzed oil transesterification with
92 subcritical methanol have been aimed at improving the process efficiency, i.e. at reducing the
93 temperature, pressure and methanol-to-oil molar ratio applied under supercritical non-catalyzed
94 vegetable oil methanolysis. Furthermore, the problem of a huge amount of waste water generated
95 during the homogeneous transesterification and biodiesel purification, could be easily avoided by
96 conducting the transesterification with subcritical methanol and an appropriate solid catalyst
97 [36].

98 Common reaction conditions for various heterogeneous catalysts at higher temperature
99 and pressure are $>150\text{ }^{\circ}\text{C}$ and $>30\text{ bar}$ [37][38][39][40] and the methanol-to-oil molar ratio
100 higher than 15:1 (methanol is in subcritical or supercritical condition) [41][42]. High temperature
101 synthesis have recently been applied with MnCO_3 , $\text{MnCO}_3/\text{Na-silicate}$ [8][9] and MnCO_3/ZnO
102 [43] catalysts in the form of powder or granules (coarse particles). Furthermore, it is worth

103 mentioning that methanol-to-oil molar ratio and reaction temperature applied in the biodiesel
104 production with MnCO_3 or $\text{MnCO}_3/\text{Na-silicate}$ catalyst were lower than those suggested by Yin
105 et al. [44] for the subcritical sodium silicate-catalyzed soybean oil methanolysis. The
106 $\text{MnCO}_3/\text{Na-silicate}$ catalyst prepared in the form of granulated particles have an acceptable
107 activity, excellent selectivity towards FAME formation from TAGs, and acceptable lifetime at
108 high temperature [9].

109 This article reports designing and testing of a pilot plant applied for the biodiesel
110 production by the soybean oil transesterification catalyzed by $\text{MnCO}_3/\text{Na-silicate}$ with the
111 capacity of 100 liters of biodiesel per day. Results of the recently reported study [9]
112 supplemented with information from several additional experiments realized in batch autoclave
113 with different amount of $\text{MnCO}_3/\text{Na-silicate}$ (5–20 wt% based on oil) at 448 K and 18:1
114 methanol to oil molar ratio, were the basis for design of packed bed tubular reactor (PBTR) as
115 main equipment of corresponding pilot plant. PBTR was filled with $\text{MnCO}_3/\text{Na-silicate}$ as
116 catalyst mixed with inert glass beads and such reactor was applied for continuous
117 transesterification at subcritical condition of methanol. Test of continuous operation was used to
118 prove designed capacity and operational characteristics of pilot plant unit during 100 hours of
119 operation. Investigation was started using PBTR filled only with glass beads for 11 h, and then,
120 the catalyzed transesterification of soybean oil with $\text{MnCO}_3/\text{Na-silicate}$ as catalyst was realized
121 during 85 h of continuous operation. Two complete mass balances were determined for detailed
122 examination of the content of produced biodiesel while sample of used catalyst after 85 h of
123 continuous process was withdrawn from reactor and its characteristics were analyzed using
124 XRD, TG/DSC and FTIR.

125 **2. Materials and methods**

126 *2.1. Catalyst preparation*

127 The preparation and characterization of the $\text{MnCO}_3/\text{Na-silicate}$ catalyst have recently
128 been reported [9]. The catalyst was activated by drying at 473 K for 2 h, followed by the
129 calcination in an oven at 773 K for 3 h.

130 2.2. Experimental procedure

131 2.3.1. Batch reactor

132 The soybean oil transesterification was conducted in 300 mL batch autoclave (AE –
133 Autoclave Engineers, USA), with an electrical heater and a Rushton-type mixer (560 rpm) at the
134 methanol to soybean oil ratio of 18:1, 448 K [45] and different $\text{MnCO}_3/\text{Na-silicate}$ catalyst
135 amounts (5, 10 and 20 wt% of the mass of oil). The reaction mixture samples withdrawn from
136 the batch autoclave was analyzed as recently described [9][45]. The standard deviation for all
137 experiments was determined to be $\pm 2.86\%$.

138 2.3.2. Pilot plant

139 A pilot plant with a PBTR, designed on the basis of the kinetic data obtained in the
140 laboratory batch reactors, was constructed and used for biodiesel production from soybean oil.
141 During the test of the pilot-plant capacity and the catalyst activity, the following parameters were
142 monitored: pressure, temperature and the mass flow rates of the reactants (methanol and soybean
143 oil) while the masses of the produced biodiesel and glycerol were measured. Two tests during the
144 continuous soybean oil transesterification were conducted:

145 1) the non-catalyzed reaction in the PBTR only filled with 2 mm glass beads for 11 h (so
146 called ZERO test) and

147 2) the catalyzed reaction in the PBTR filled with a mix of 2 mm glass beads and catalyst
148 particles ($0.99 < d < 1.99$ mm) in the proportion 60:40 by weight for 85 h (so called LONG
149 TERM test, $LT-t$).

150 2.3.3 Catalyst characterization

151 The properties of the used catalyst (withdrawn from the PBTR after 85 h of continuous
152 operation) were characterized by X-ray diffraction (XRD) on a Philips PW 1050 X-ray powder
153 diffractometer using Ni-filtered $\text{Cu K}\alpha_{1,2}$ ($\lambda = 1.54178 \text{ \AA}$) radiation with a scanning step width of
154 0.05° and a counting time of 3 s per step, thermal analysis (TG/DTA) on a Setaram Instrument
155 between 293 K and 1273 K in air flow (20 K min^{-1}) and Fourier transformed infrared
156 spectroscopy (FTIR) using a BOMEM spectrometer (Hartmann & Braun) in the wave number
157 range of $4000\text{--}400 \text{ cm}^{-1}$ with 4 cm^{-1} resolution.

158 3. Results and discussion

159 3.1. Analysis of soybean oil transesterification in a batch reactor

160 The soybean oil transesterification in the presence of the MnCO_3/Na -silicate catalyst
161 occurs via two simultaneous catalytic processes [9]: one is catalyzed heterogeneously by both
162 active species (Mn and Na) fixed on the surface of solid catalyst particles and homogeneously by
163 Na dissolved in the esters and methanol/glycerol phases. It is important to point out that the
164 batch transesterification reaction takes place during the heating of the reaction mixture from the
165 room temperature to the specified reaction temperature (non-isothermal regime), and while
166 keeping the reaction temperature constant (isothermal regime). The apparent reaction rates are
167 simply defined by the reaction rate constants, k_{LT} and k_{HT} , depending on the reaction temperature
168 and determined for the process performed with 5 wt% of the catalyst (based on the oil) [9]:

169 For the isothermal operation at $T < 423$ K

$$170 \quad k = k_{\text{LT}} = 7.918 \exp(-2465 / T), \text{ min}^{-1} \quad (1a)$$

171 For heating above 423 K and the isothermal transesterification at $T > 423$ K

$$172 \quad k = k_{\text{HT}} = 6.355 \times 10^5 \exp(-7272 / T), \text{ min}^{-1} \quad (1b)$$

$$173 \quad k = k_{\text{LT}} = 7.918 \exp(-2465 / T), \text{ min}^{-1} \quad \text{for } T < 423 \text{ K} \quad (1a)$$

$$174 \quad k = k_{\text{HT}} = 6.355 \times 10^5 \exp(-7272 / T), \text{ min}^{-1} \quad \text{for } T > 423 \text{ K} \quad (1b)$$

175 The rate of TAG conversion was defined by the following kinetic equation [9]:

$$176 \quad \frac{dx_{\text{TAG}}}{dt} = k_{\text{app}}(1 - x_{\text{TAG}}) \quad (2)$$

177 where k_{app} , according to the IL kinetic model, is defined as follows:

$$178 \quad k_{\text{app}} = \frac{k \cdot k_{\text{mt}}}{k + k_{\text{mt}}} = \frac{k_{\text{app}} \cdot k_{\text{mt}0} \cdot [1 + \alpha(x_{\text{TAG}})^\beta]}{k_{\text{app}} + k_{\text{mt}0} \cdot [1 + \alpha(x_{\text{TAG}})^\beta]} \quad (3)$$

179 The best agreement between the calculated and experimentally determined TAG
180 conversion degrees was obtained using the values of the reaction rate constant k (i.e. k_{LT} or k_{HT}),
181 the initial value of the mass transfer coefficient $k_{mt0} = 0.085 \text{ min}^{-1}$, and the values of the
182 parameters $\alpha = 55$ and $\beta = 3.5$ [9].

183 3.2. Analysis of the transesterification in the batch reactor performed with different amounts of 184 catalyst

185 In the present study, several experiments were conducted in the AE batch reactor using
186 5%, 10% and 20% of $\text{MnCO}_3/\text{Na-silicate}$ catalyst based on mass of oil (particle size 0.99–1.99
187 mm) at 448 K to verify the proposed IL kinetic model at higher catalyst amounts [9]. Besides,
188 unlike previously reported results [9] the isothermal temperature of 448 K in this study was
189 reached in the batch autoclave for 113 min. The difference in the heating time needed to reach
190 the isothermal transesterification temperature in the batch autoclave could give additional
191 information about the flexibility of the proposed IL kinetic model used to predict TAG
192 conversion at 448 K.

193 The experiments with 5% of catalyst (based on oil) showed that the TAG conversion of
194 62.6% was obtained during heating period of 113 min (54.6% for 54 min [9]), while TAG
195 conversion of 81.3% and 98.2% were obtained with 10% and 20% of catalyst, respectively for
196 the same time of non-isothermal heating. Further 1 h of isothermal transesterification at 448 K
197 with 5% and 10% of catalyst gave almost the complete TAG conversion (>99%). According to
198 these data the following recalculations of the reaction apparent rate constant k (i.e. k_{LT} and k_{HT})
199 and mass transfer coefficient k_{mt0} , which depended on the total catalytic surface area [8], were
200 used to determine the reaction rate constant k_{app} applicable for both non-isothermal (heating to
201 448 K) and isothermal regime:

$$202 \quad k_{(w)} = k_{(5)} \frac{C_{cat(w)}}{C_{cat(5)}} \quad (4a)$$

203 and

$$204 \quad k_{mt0(w)} = k_{mt0(5)} \frac{C_{cat(w)}}{C_{cat(5)}} \quad (4b)$$

205 thus leading to:

$$206 \quad k_{app(w)} = k_{app(5)} \frac{c_{cat(w)}}{c_{cat(5)}} \quad (4c)$$

207 where $c_{cat(w)}$ is the catalyst amount used for the transesterification of soybean oil (valid for $2 < w$
208 < 8 wt% based on the mass of oil).

209 Furthermore, recently reported results showed only a slight increase of TAG conversion
210 (to 95%) during heating to 428 K and 1 h of isothermal transesterification at 428 K with
211 increasing the catalyst amount from 8 to 13% [9], which implied that the apparent reaction rate
212 constant ($k_{app(w)}$) depended almost linearly on the catalyst concentration only in the range of
213 catalyst amount between 2% and 8%, as shown by Eq. (4).

214 The relation between $k_{app(w)}$ and catalyst concentration might deviate from the linear
215 dependence (valid for $5 < w < 8$, Table 1), when larger catalyst concentrations are used. Namely,
216 the apparent reaction rate constant $k_{app(w)}$, as a “lumped parameter”, includes the resistance of
217 TAG mass transfer to the surface of catalyst particles and the resistance of chemical reaction
218 between TAGs and methoxide ions at the catalyst surface. These resistances have different and
219 specific relation to temperature and catalyst concentration. The mass transfer coefficient is
220 related to square root of temperature ($T^{0.5}$) while the chemical reaction rate constant is an
221 exponential function of temperature according to the Arrhenius equation. Also, the resistance of
222 chemical reaction can be correlated directly to the catalyst concentration (i.e. to the available
223 catalyst surface area) while the resistance of mass transfer depends on the hydrodynamic
224 conditions in the reactor (mixing, viscosity). Therefore, the relation between $k_{app(w)}$ and catalyst
225 concentration may be non-linear, as shown in some recently reported investigations [8].

226 While the linear correlation between $k_{app(w)}$ and catalyst concentration was assumed for
227 the catalyst concentration between 2 and 8%, a different correlation was proposed for the catalyst
228 concentration higher than 8% (i.e. 10% and 20% in this study) according to relation:

$$229 \quad k_{app(w)} = \varphi k_{app(5)} \quad (5a)$$

$$\varphi = 1.6 \left[2 - \exp\left(\frac{8-w}{8}\right) \right] \quad (5b)$$

231 which means that the maximal increase of the apparent reaction rate constant might be 2 times
 232 related to the value determined or 3.2 times higher than the value valid when 8% or 5% of
 233 catalyst is used, respectively. Thus, for the experiments conducted in the batch autoclave (300
 234 mL, 560 rpm), the corresponding values of k_{app} and two other kinetic model parameters ($\alpha = 55$
 235 and $\beta = 3.5$, accepted from the previous work [9]) were used for calculation and comparison with
 236 the experimentally determined TAG conversions (Table 1).

237 **Table 1.** Experimental results of the soybean oil transesterification during non-isothermal
 238 heating from 288 K to 448 K and subsequent isothermal heating at 448 K for 1 h.

M_{cat} , based on the mass of oil (wt%)	Operation regime	Time (min)	Temperature (K)	$x_{TAG, exp}$ (%)	$x_{TAG, calculated}$ (%)	
					After 113 min	At the end of isothermal operation
5	Heating	113	288→448	62.6	66.9	–
	Isothermal operation	60	448	98.3	–	98.8
10	Heating	113	288→448	81.3	88.7	–
	Isothermal operation	60	448	97.2	–	99.9
20	Heating	113	288→448	98.2	95.9	–
	Isothermal operation	60	448	99.9	–	100

239 An excellent agreement between the calculated and experimentally determined TAG
 240 conversions at the end of non-isothermal heating (113 min) and the end of the overall process
 241 was observed as confirmed by small mean relative percentage deviations (4.4% and 1.6%,
 242 respectively). These results proved the proposed and used correlation between the apparent
 243 reaction rate constant and the applied catalyst amount and validated the kinetic parameters
 244 involved in the IL kinetic model.

245 3.3. Design of packed bed tubular reactor

246 Since the methanolysis reaction was performed in the batch stirred reactor with perfect
247 mixing, the design equation coming out from the mole balance of TAG is the same for the PBTR
248 with ideal plug flow. In order to calculate the residence time of the reaction mixture in the pilot
249 PBTR operating under adiabatic condition, the following differential equations of mole and
250 energy balances were applied:

251
$$\frac{dx_{TAG}}{d\tau} = k_{app}(1 - x_{TAG}) \quad (6)$$

252
$$\frac{dT}{dx_{TAG}} = -\frac{F_{TAG,0}\Delta H_r}{m_0 c_p} \quad (7)$$

253 Using Eqs. (5a) and (5b) and assuming that the catalyst-to-oil mass ratio in the reactor
254 would be much higher than 20%, the following equation, that connects reaction rate constant
255 with temperature, was used to calculate the k_{app} values:

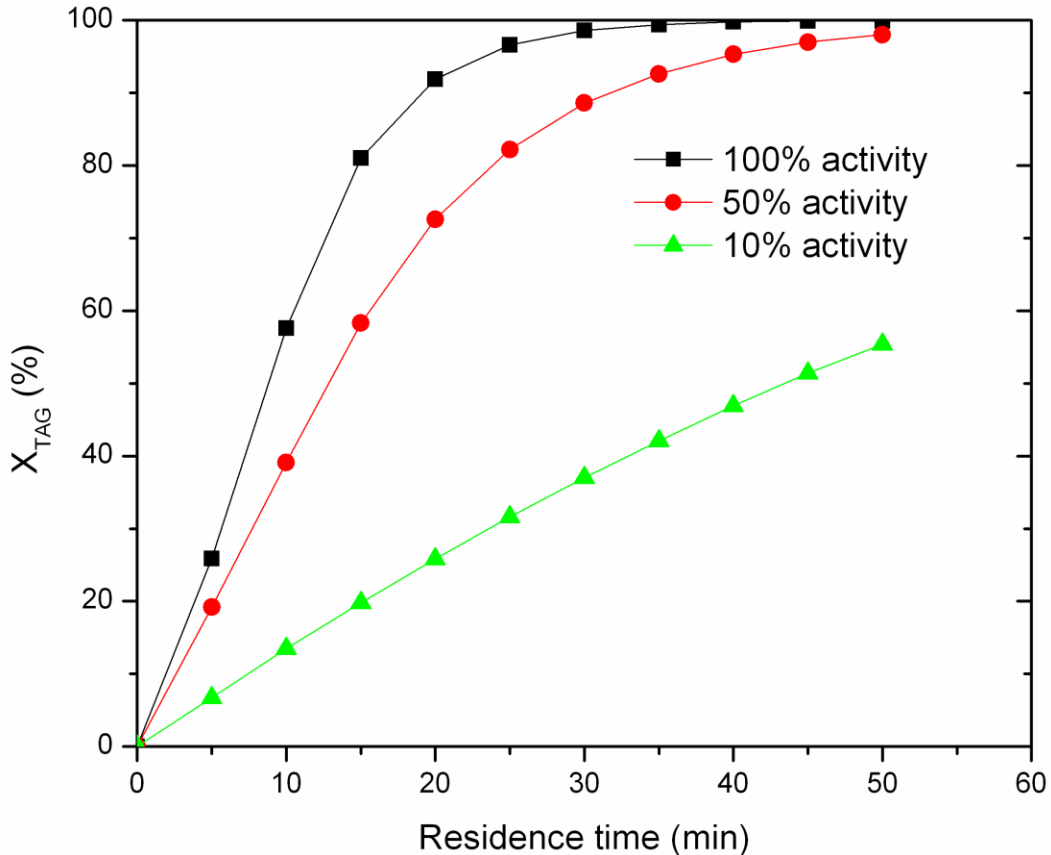
256
$$k = 3.2 \cdot k_{HT(w=5\%)} = 2.034 \times 10^6 \exp\left(-\frac{7272}{T}\right), \text{ min}^{-1} \quad (8)$$

257 Simultaneous solution of Eqs. (6) and (7) for the initial condition:

258 $x_{TAG} = 0$ for $\tau = 0$ and $T(0) = T_{in} = 443$ K

259 gave the TAG conversion degree, x_{TAG} , and the temperature at the outlet of the reactor, T_{ex} , for
260 the residence time of $\tau = 50$ min. The values of the specific heat, c_p , and the heat of reaction, ($-$
261 ΔH_r), were taken from the literature [46].

262 For the initial activity of catalyst (100%), almost complete TAG conversion ($x_{TAG} = 1$ or
263 100%) could be obtained at the outlet of the reactor after 50 min of residence time. If the catalyst
264 activity in the PBTR dropped to 50% of its initial value, then the TAG conversion degree at the
265 reactor outlet would be 98%. Further decrease of the average catalyst activity in the PBTR, e.g.
266 to 10% of its initial activity would result in 55% TAG conversion degree, as shown in Fig. 1.



267
 268 **Fig. 1.** Conversion degree versus residence time of the reaction mixture for different
 269 average catalyst activities in the PBTR.

270 The design of the PBTR having capacity of 100 L/day was based on the following
 271 assumptions:

- 272 • The process efficiency of 90% was adopted, resulting the biodiesel production capacity of
 273 4.17 kg/h (0.07 kg/min).
- 274 • For the complete conversion of soybean oil (>99%), the inlet soybean oil (TAG) mass flow
 275 rate ($m_{o,TAG}$) should be 4.17 kg/h.
- 276 • Taking into account the molar masses of soybean oil (890 g/mol) and methanol (32 g/mol)
 277 and their molar ratio of 1:18, the inlet concentration of TAGs, represented by triolein as a key
 278 compound (c_{TAGo}) would be 0.60 mol/L, while the molar and mass flow rates of the reaction
 279 mixture (M_o and m_o) into the PBTR would be 89 mol/h and 6870 g/h, respectively; the inlet
 280 TAG molar flow rate of (F_{TAGo}) was 4.68 mol/h.

- 281 • The catalyst bed would be prepared by mixing $\text{MnCO}_3/\text{Na-silicate}$ catalyst particles (bulk
282 density of 1.2 g/mL) and inert glass beads (2 mm; 2.5 g/mL) with the mass ratio of 40:60.
283 • The porosity of the catalyst bed was assumed to be 50%.
284 • The proposed residence time of the reaction mixture in the PBTR would be 50 min.
285 • The reaction mixture would be heated in a preheater to 448 K to the reaction temperature in
286 the PBTR.
287 • The inlet mass flow rates of the soybean oil and methanol would be 6870 g/h or 8.6 L/h,
288 corresponding to the methanol-to-oil molar ratio of 18: 1.
289 • The density of the reaction mixture at 448 K and 25 bar was assumed to be about 800 kg/L.
290 • A simple calculation gave the volume of the reaction mixture which occupied the void space
291 of the bed of 7.16 L and the volume of the empty reactor of 14.33 L. Thus, the reactor could
292 be packed with 8.33 L of $\text{MnCO}_3/\text{Na-silicate}$ catalyst (or 10 kg; density 1.2 kg/L) and 6 L of
293 inert glass beads (spheres) (15 kg; density of 2.5 kg/L).
294 • The amount of oil in the reactor would be 3.90 kg, so the catalyst concentration (based on the
295 mass of oil) in the reactor would be $10/3.90 = 2.56$ kg/kg or 256%.

296 The final design of the PBTR was based on the following:

- 297 a. Volume of the tubular reactor would be 14 L.
298 b. Mass of 10.2 kg of catalyst particles (cylindrical granules with the average diameter between
299 0.9 and 1.99 mm) and mass of 15.3 kg of glass beads (2 mm), respectively should be used for
300 preparing the packed bed.
301 c. The biodiesel production capacity would be 4.05 kg/h or 97 kg/day, i.e. slightly above 100
302 L/day (density of biodiesel: 0.9 kg/L).

303 3.4. Assessment of catalyst deactivation during long-term continuous operation

304 The catalyst activity in the successive batches was evaluated in the batch autoclave with
305 the same amount of catalyst (10 wt% based on the oil weight) at 458 K and with the 30:1
306 methanol-to-oil molar ratio [9]. It was found that the catalyst might be reused 8–9 times without
307 substantial decrease of the TAG conversion degree (from 100% to 97.4%) but with the change of
308 FAME yield from 99%, to 92.6% and 88.3% after 8th and 9th catalyst reuse, respectively [9].

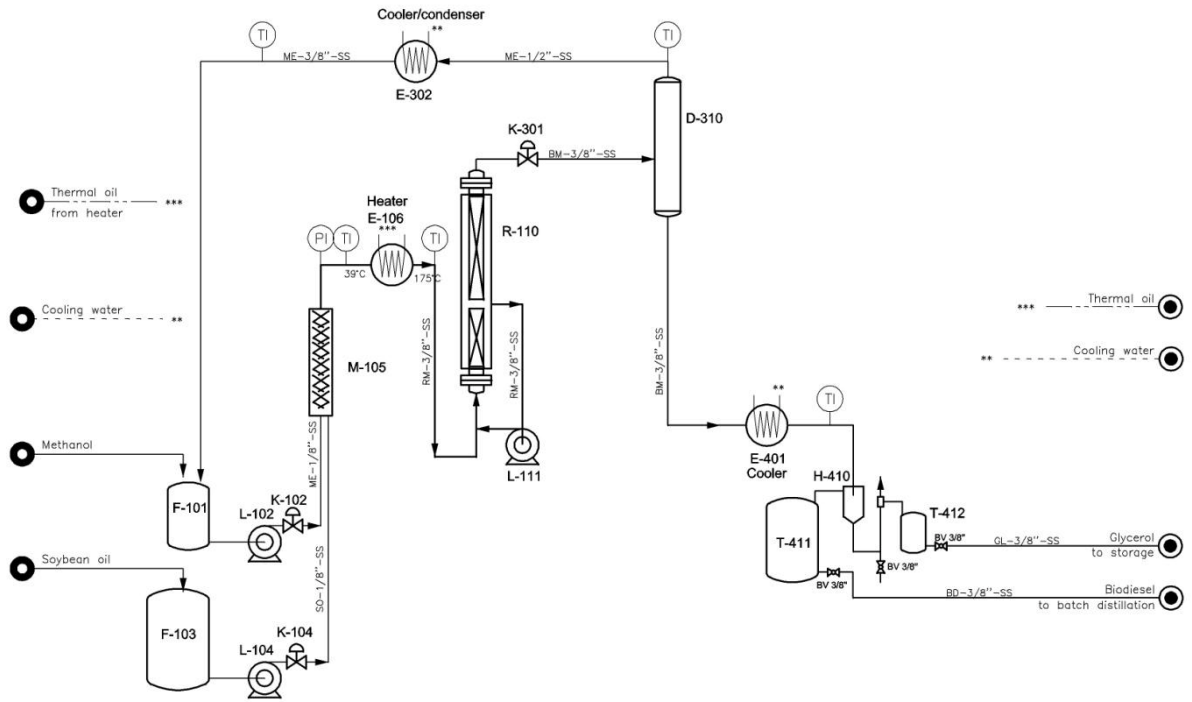
309 Therefore, 10 kg of the catalyst placed in the PBTR could be used for processing 800 kg of
310 soybean oil. In other words, the catalyst might be used for 8-day continuous operation of the
311 PBTR when TAG conversion degree would be slightly decreased to 97.4%. However, the
312 catalyst activity after 8 days of continuous operation would be only 35% of the initial activity.

313 **4. Pilot plant design**

314 The main steps of the proposed continuous biodiesel production are the mixing of oil and
315 methanol and preheating their mixture to the reaction temperature, the transesterification of
316 soybean oil in the PBTR, the separation of the excess of methanol, the separation of biodiesel
317 and glycerol and the purification of biodiesel and glycerol. In order to reduce the overall
318 investment and operational costs of the pilot plant operation, only the capacity of the pilot plant
319 was tested while the downstream glycerol and biodiesel purification was not considered at the
320 present stage of the pilot plant construction. Hence, the main process scheme included:

- 321 • pumping, mixing and preheating of methanol and oil;
- 322 • flowing of the soybean oil/methanol mixture into the PBTR;
- 323 • flash separation of the excess of methanol from the reaction mixture; and
- 324 • separation of biodiesel (upper) and glycerol (lower) layer.

325 The process flow sheet with the main streams and units is shown in Fig. 2a while the
326 photo of the pilot plant is presented in Fig. 2b. The main equipment units of the pilot plant are
327 specified in Table 2.



328

329

(a)



330

331

(b)

332

Fig. 2. The pilot plant for FAME synthesis: (a) layout and (b) photo.

333

Table 2. The main units of pilot plant.

Unit	Used as	Dimensions	Volume
F-101	Storage tank for oil	$\text{Ø}600 \times 1200 \text{ mm}$	0.4 m^3
F-103	Storage tank for methanol	$\text{Ø}450 \times 1000 \text{ mm}$	0.176 m^3
M-105	Static mixer	DN15	–
E-106	Preheater	380 V, 10 kW	–
R-110	Reactor	$\text{Ø}133 \times 5 \text{ mm}$ H = 1400 mm	0.019 m^3
D-310	Flash evaporator	$\text{Ø}159 \times 4 \text{ mm}$ H = 500 mm	0.01 m^3
E-302	Condenser for methanol	A = 0.004 m^2	–
E-401	Cooler of FAME–glycerol mixture	A = 0.008 m^2	–
T-411	Separator	$\text{Ø}159 \times 4 \text{ mm}$ H = 300 mm	0.006 m^3
F-104	Storage tank for FAME	$\text{Ø}600 \times 1200 \text{ mm}$	0.33 m^3
F-105	Storage tank for glycerol	$\text{Ø}377 \times 500 \text{ mm}$	0.06 m^3

334

The proposed operation conditions for the biodiesel production in the pilot plant facility

335

were the methanol to soybean oil molar ratio of 18:1, the reaction temperature of 448 K and the

336

maximal working pressure of 30 bar. The minimal TAG conversion degree achieved in the

337 PBTR after 8th day of the use the MnCO₃/Na-silicate catalyst was assumed to be 97.4%. After 8
338 days of continuous operation, the catalyst must be replaced by a packed-bed of fresh catalyst.

339 *4.1. Analysis of operating parameters*

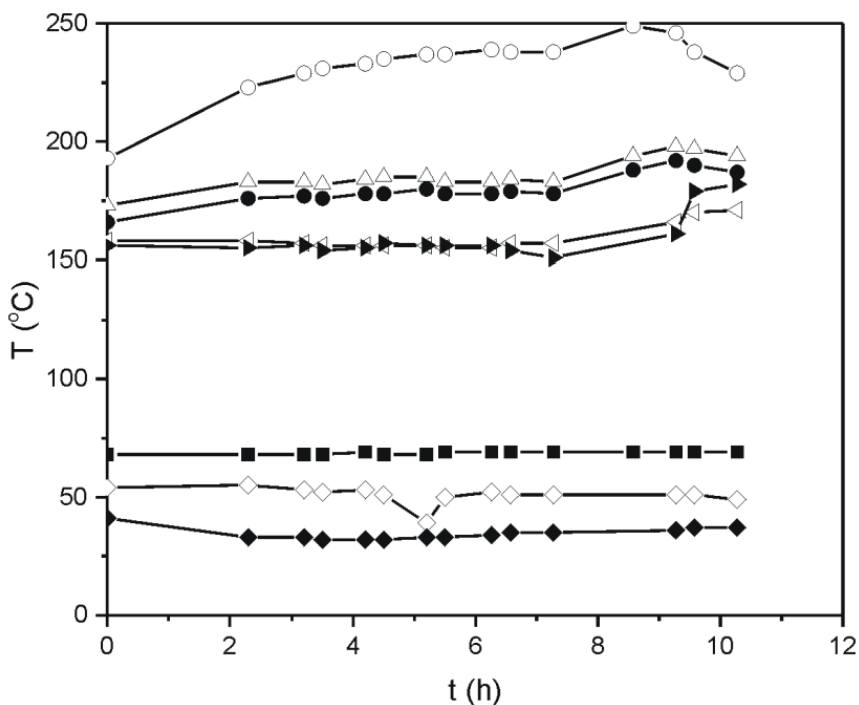
340 The main objectives of testing the pilot plant were to investigate the soybean oil
341 methanolysis catalyzed by MnCO₃/Na-silicate for the biodiesel production under the conditions
342 established in the laboratory batch reactor and to prove the designed capacity of the pilot plant.

343 *4.1.1. Pilot plant testing*

344 First, the pilot plant was tested on the leakage and the pressure by flowing the tap room
345 temperature water (so-called cold test) and then soybean oil preheated in the preheater to 175 °C
346 (448 K) at the flow rate of 6.3 L/h (maximum capacity of the pump). The pilot plant comprised
347 the system for monitoring (measuring and manual control) temperature of the heater, the reactor
348 (inside the packed bed, in the jacket and the reactor outlet), the flash evaporator, the condenser
349 and the cooler as well as the system for measuring the pressure at the inlet and outlet of the
350 reactor.

351 *4.1.2. Non-catalyzed FAME synthesis in pilot plant (ZERO test)*

352 After passing through the static mixer (M-105) and the preheater (E-106), methanol and
353 soybean oil were pumped into the PBTR (R-110). The residence time of the reaction mixture in
354 the preheater and the connecting pipeline between the preheater and the PBTR enabled only a
355 minimal effect of the non-catalyzed transesterification [36]. The variation of temperature, which
356 was controlled at several points of the pilot plant, during 11 h of the non-catalyzed FAME
357 synthesis is shown in Fig. 3.



358

359 **Fig. 3.** Variations of temperature at the measuring points during the non-catalyzed synthesis of
 360 FAMEs (thermal oil at the heater inlet – ○; the reactants' mixture at the heater outlet – ●; the
 361 reactor – △; the reactor jacket – ◁; the reactor outlet – ►; the evaporator – ■; the condenser –
 362 ◇; and, the cooler – ◆).

363 The temperature of the reactants leaving the preheater was slightly higher than the
 364 desired reaction temperature of 175 °C as well as the temperature inside the reactor. However,
 365 the measured temperature of the reaction mixture at the reactor outlet was about 155 °C at the
 366 beginning of the non-catalyzed (so-called ZERO test). This was attributed to the temperature
 367 sensor position which was mounted on the outside surface of the reactor wall. The detected
 368 temperature at the top of the flash evaporator was lower than the desired one (>80 °C), which
 369 was explained also by the position of the temperature sensor which was placed on the outside
 370 surface of the evaporator. The temperatures in the condenser and the cooler were relatively
 371 stable.

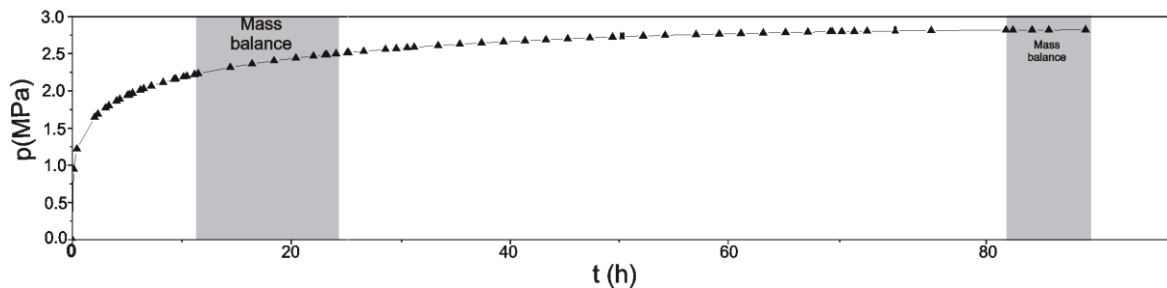
372 The contents of FAMEs, TAGs, DAGs and MAGs in the samples of the reaction mixture
 373 taken at the outlet of the heater (inlet into the reactor) and the outlet of the reactor during the
 374 ZERO test ($t = 0, 3, 7, 9$ and 11 h) were determined. Only the presence of about 6% of DAGs

375 and a negligible concentration of MAGs (0.7%) were detected in the samples at the inlet of the
376 reactor. These data indicate that the reaction started even in a relatively short residence time of
377 the reactants in the heater and the connecting pipeline. The HPLC analysis of the esters phase
378 separated from the samples taken at the outlet of the reactor showed the following average
379 contents: 60% of TAGs, 22.5% of FAME or biodiesel, 11.5% of DAGs and 6% of MAGs during
380 11 h of non-catalyzed transesterification. Thus, for the applied residence time of oil in the empty
381 tubular reactor, the non-catalyzed conversion of TAGs of about 40% was achieved and that
382 about 50% of TAGs were converted into FAMEs.

383 4.1.3. Catalyzed synthesis of FAMEs in the PBTR (Long Term test, *LT-t*)

384 After the non-catalyzed reaction was completed, the reactor was discharged, and filled
385 with catalyst particles and glass beads (mass ratio of 2:3; 10 kg of $\text{MnCO}_3/\text{Na-silicate}$ catalyst
386 and 15 kg of glass beads; 0.51 was experimentally determined porosity of catalyst bed).
387 Methanol and soybean oil were heated to 175 °C and kept at this temperature for 30 min. After
388 that, the mixture of the preheated reactants was fed to the reactor bottom. The temperature of the
389 reaction mixture (mainly soybean oil and methanol) at the outlet of the preheater was close to the
390 temperature inside the reactor and did not exceed 190 °C, thus preventing the overheating of
391 soybean oil and the unwanted side reactions (e.g. polymerization). This temperature was
392 achieved with the temperature of heating oil in the heater in the range from 180 °C to 210 °C
393 (Fig. 4b). The average pressure in the reactor was 2.5 MPa during the *LT-t* and slightly lower
394 during the FIRST mass balance of the *LT-t*, compared to the average pressure during the
395 SECOND mass balance of the *LT-t* (Fig. 4a). The temperature inside the PBTR varied in the
396 range from 175 °C to 195 °C (Fig. 4b).

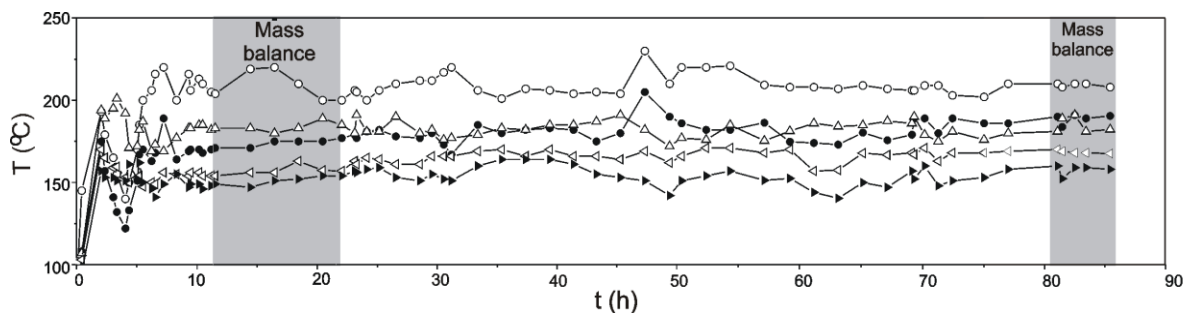
397



398

399

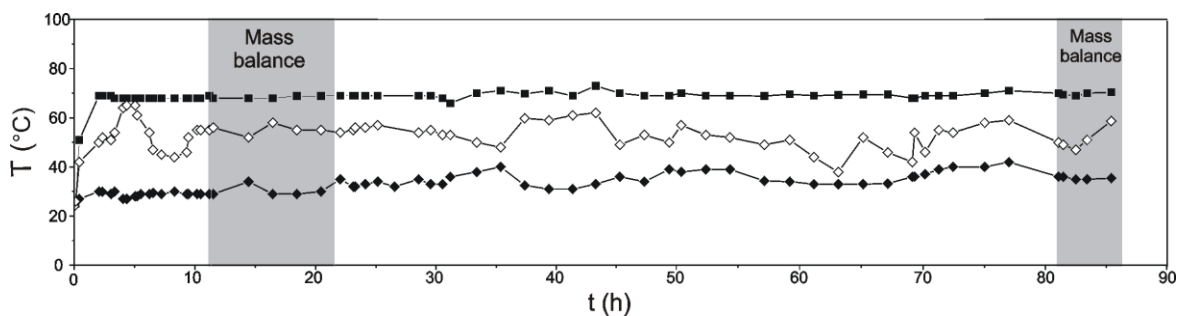
(a)



400

401

(b)



402

403

(c)

404 **Fig. 4.** Variation of pressure and temperature: (a) \blacktriangle – pressure at reactor inlet measured at the
 405 pump; and temperature measured at different points during the LONG TERM experiment, (b) \circ
 406 – thermal oil at the heater inlet, \bullet – the reactants' mixture at the heater outlet, \triangle – reactor, \triangleleft –
 407 jacket, \blacktriangleright – outlet of reactor; (c) \blacksquare – evaporator, \diamond – condenser, \blacklozenge – cooler.

408 Considering the methanol-to-oil molar ratio (18:1 and 25:1) employed in this process
 409 during the FIRST and SECOND mass balances, certain difficulties in the separation of the final
 410 products could be expected. Therefore, the flash evaporator (D-310, Fig. 2a) was included in the
 411 pilot plant facility, where the excess methanol from the outlet reaction mixture was removed by
 412 partial vaporization, enhancing the separation between esters and glycerol phases due to their
 413 poor mutual solubility. The temperature of 69 °C in the flash evaporator used for removing the
 414 excess of methanol from the ester and glycerol mixture was constant (Fig. 4c). After the flash
 415 evaporation step, the outlet stream of the main transesterification products, consisting of esters
 416 and glycerol phases, pass through the cooler to a gravitational separator.

417 Generally, the measured temperatures at the outlet of the preheater, the inlet and outlet of
 418 the reactor, as well as at the surface of the flash evaporator, were stable, without extreme
 419 fluctuation. However, the pilot plant did not have the system for automatic control of
 420 temperature in the reactor, so it was regulated manually, thus making difficult to maintain stable
 421 both the pressure and the temperature in the reactor at the desired levels, as can be seen in Fig. 4.

422 Two complete mass balances were realized (highlighted area in Fig. 4) aimed at
 423 determining the actual mass flow rates of the reactants and the products and the composition of
 424 biodiesel after its separation from glycerol. The masses of different fractions were collected at
 425 inlet and outlet of the reactor during the FIRST (between 11th and 21th h of operation) and
 426 SECOND (between 81th and 86th h of operation) mass balance and measured on scale; the
 427 obtained masses are presented in Table 3 while the composition of esters phase determined by
 428 HPLC analysis is shown in Table 4.

429 **Table 3.** Mass balances realized during the Long Term test (*LT-t*).

Mass balance experiment	INLET		OUTLET		
	Oil (kg)	Methanol (kg)	Raw ester phase (kg)	Raw glycerol phase (kg)	Recovered methanol (kg)
FIRST	31.91	20.64	32.75	9.55	10.25
SECOND	11.2*	10*	12.56	2.75	5.89

430 * The value of methanol –to-oil molar ratio during the 2nd mass balance was changed to 25:1.

431 **Table 4.** The average composition of the ester phase.

Mass balance	FAME (%)	MAG (%)	DAG (%)	TAG (%)
FIRST	98.56	0.53	0.91	0.00
SECOND	97.49	1.08	1.21	0.22

432 The samples of crude ester and glycerol phases (1 L each) collected during the mass
 433 balance checking were left to stay for 2 days. The phases were separated and the following layers
 434 were detected:

- 435 • The crude esters sample (vol%): the FAME phase (upper layer) about 93% and the
436 glycerol phase (lower layer) 4% while the evaporated methanol was approximately 3%.
- 437 • The crude glycerol sample (vol%): methanol (upper layer) 3.2%, FAME phase (middle
438 layer) 2.5% and lower layer 87.3% as a mixture of glycerol (80.3 %) and methanol (7%).

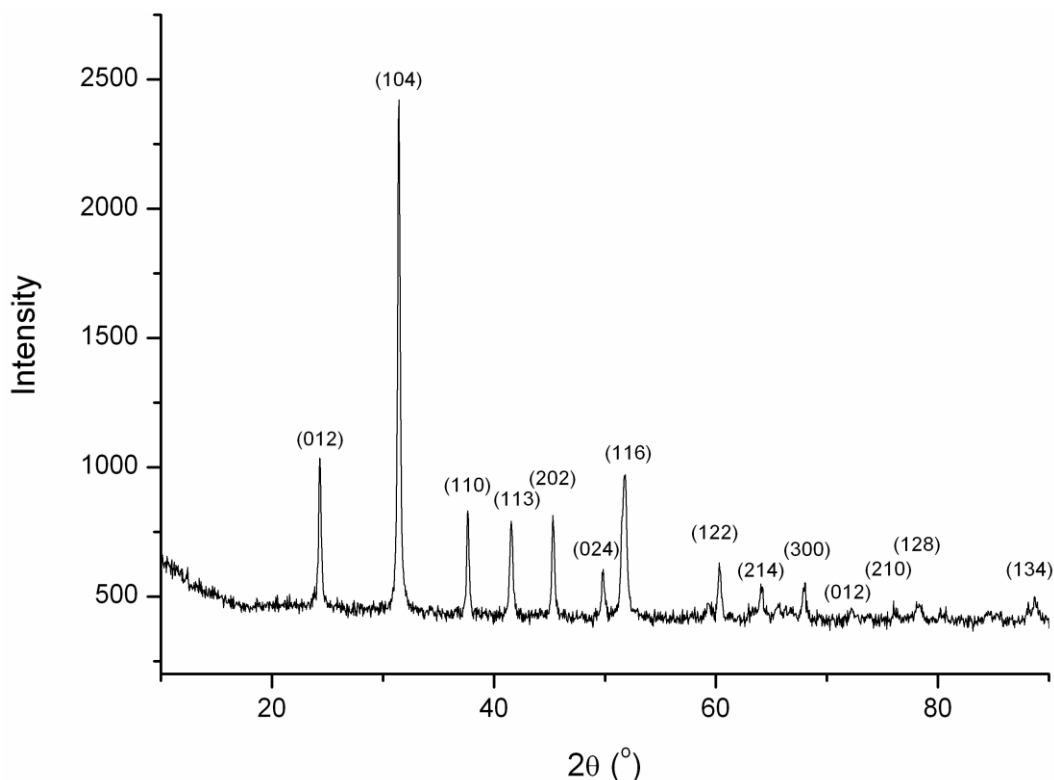
439 Based on this observation, it might be concluded that the final products collected during
440 the FIRST mass balance contained 30.8 kg of pure ester phase (30.4 kg of FAMEs and 0.4 kg of
441 DAGs and MAGs), 0.09 kg of methanol and 1.83 kg of glycerol.

442 This analysis showed that the FAME content was very high in the esters phase analyzed
443 during the *LT-t* (Table 4). In both mass balances FAME content was higher than 96.5%, meeting
444 the requirements of the biodiesel standard specifications (EN 14214). It was worth mentioning
445 that during the *LT-t*, the contents of DAGs and MAGs were very low, but still slightly higher
446 than those defined by standards (0.2% for DAG and 0.8% for MAG). TAGs were not detected in
447 the esters phase of the FIRST mass balance but they started to appear at the end of the SECOND
448 mass balance of *LT-t*, being close to the standard limit (0.2%). Although the conversion of TAGs
449 was still very high (99.8%), the yield of FAME dropped to 97.5%. This result agreed with the
450 observed changes in the esters phase composition during the soybean oil transesterification in the
451 repeated use of the catalyst in the batch transesterification [9].

452 4.1.4. Catalyst deactivation during Pilot Plant experiment

453 During 85 h of the *LT-t*, a small fluctuation of the esters phase composition was
454 observed. However, there were no enough data to predict exactly the catalyst deactivation during
455 85 h of its use. The simple calculation, mentioned above based on data collected in the batch
456 process, indicated that the used amount of $\text{MnCO}_3/\text{Na-silicate}$ catalyst (10 kg) would be active
457 for at least 8–9 days of the continuous process and the data of *LT-t* supported this expectation. At
458 the same time, a gradual increase of the pressure in the PBTR was observed (Fig. 4a). The
459 pressure should be enhanced for keeping the capacity of the pilot plant at the designed value,
460 which was attributed to the blocking of the interparticle space with TAGs and the side products
461 formed at a high temperature as a result of the oil polymerization.

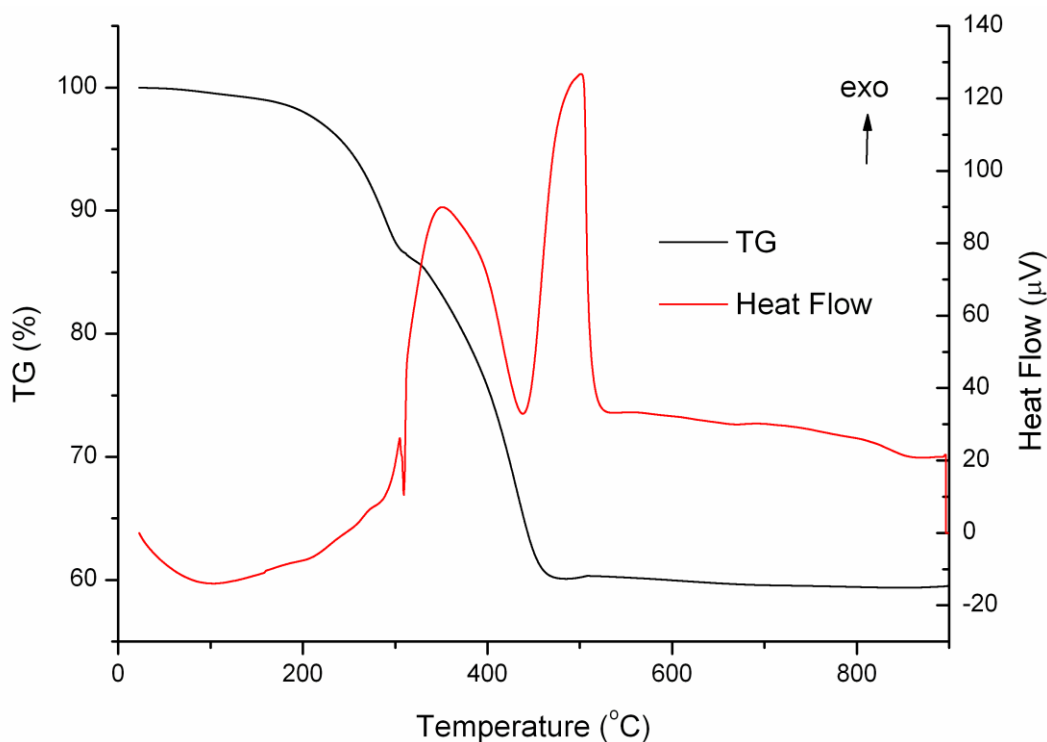
462 For defining the actual status of the used catalyst in the PBTR after the *LT-t*, the samples
463 were withdrawn from the bottom and the middle part of the PBTR and analyzed by XRD,
464 TG/DTA and FTIR. Figure 5 shows the XRD pattern of the $\text{MnCO}_3/\text{Na-silicate}$ sample (washed
465 and centrifuged with ethanol).



466
467 **Fig. 5.** XRD pattern of the $\text{MnCO}_3/\text{Na-silicate}$ catalyst taken from the middle part of the
468 PBTR after 85 h of the *LT-t* performed at 175 °C and 2.5 MPa.

469 The presence of rhombohedral structure of MnCO_3 was consistent with the literature
470 values (JCPDS Card 83-1763). Since the XRD pattern was very similar to the XRD pattern of
471 the fresh catalyst [9] it was concluded that the catalyst did not undergo any noticeable structural
472 changes during the 85 h of the *LT-t*.

473 Thermal behavior of the as-taken (without washing) $\text{MnCO}_3/\text{Na-silicate}$ is shown in Fig.
474 6.



475

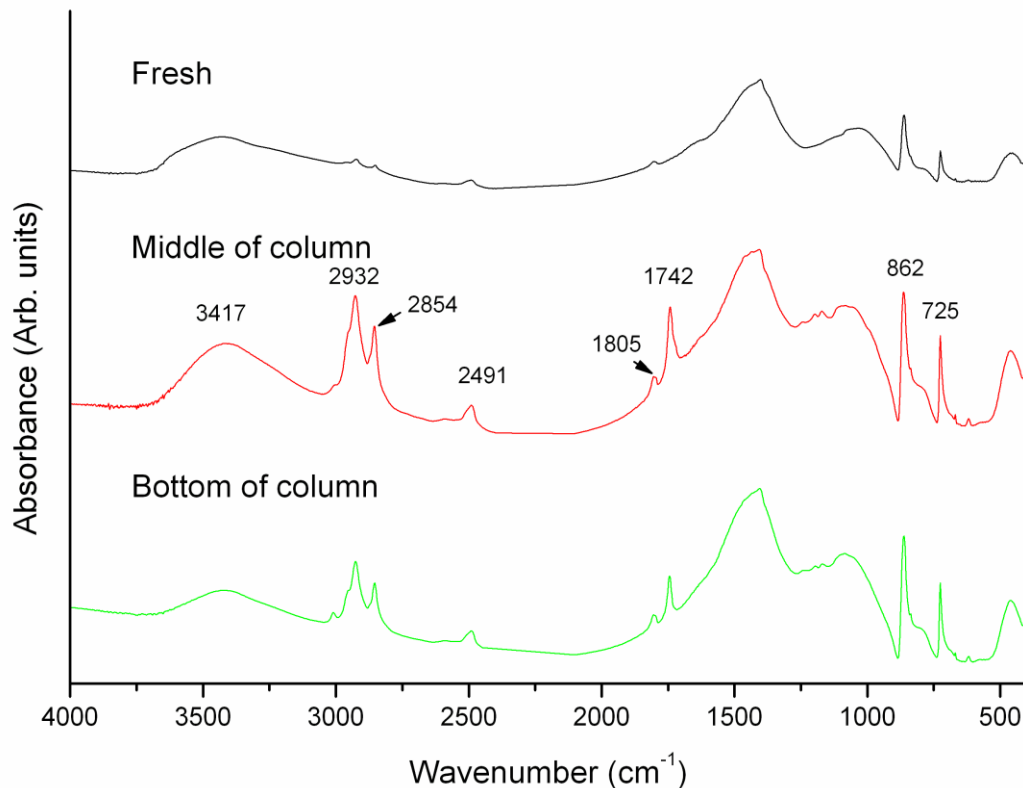
476

477 **Fig. 6.** TG/DTA analysis (heating rate: 20 K/min) of the $\text{MnCO}_3/\text{Na-silicate}$ catalyst sample
 478 taken from the middle part of the PBTR after 85 h of the *LT-t*.

479 The mass change indicated a weight loss at about 320 °C (16%), which might be
 480 attributed to the release of crystalline water and the compounds adsorbed on the catalyst surface
 481 (composed of FAMES, glycerol, and traces of TAGs, DAGs and MAGs). The second mass
 482 change was observed in the temperature range from 320 to 500 °C, with an endothermic peak at
 483 about 440 °C. It might be attributed to the thermal decomposition of MnCO_3 as well to the
 484 degradation of the reactants and the products. The total weight loss was about 40%, which was
 485 10% higher than that found for the fresh catalyst [9]. Therefore, it was concluded that a part
 486 (10%) of oil phase was adsorbed on the catalyst surface.

487

The FTIR spectra of the fresh and used catalysts are shown in Fig. 7 for comparison.



488

489 **Fig. 7.** FTIR spectra of the fresh and used catalyst collected from the bottom and middle part of
 490 the PBTR after 85 h of the *LT-t*.

491 The broad band of the spectra with the maximum at about 3400 cm^{-1} might be attributed
 492 to the hydrogen (H)-bonded stretching vibration of the O–H group, and could be assigned to the
 493 water (moisture) adsorbed from air and/or the reaction mixture on the catalyst surface. The peaks
 494 at 2932 , 1742 and 725 cm^{-1} might be assigned to C–H, C–O and C–C functional groups,
 495 respectively, while the peak at 862 cm^{-1} corresponded to the bending vibration of CO_3^{2-} in
 496 MnCO_3 .

497 It was found that the absorbance values from the wavelength region of $3700\text{--}3075\text{ cm}^{-1}$
 498 might be used for estimating the moisture content in the biodiesel samples [47]. The broad peak
 499 in this region was more pronounced for the samples taken from the middle and bottom parts of
 500 the reactor than that of the fresh sample suggesting the presence of water in the reaction mixture.
 501 Furthermore, remarkably higher intensities of the peaks at 2932 , 2854 and 1742 cm^{-1} for the

502 samples of the used catalyst, compared to that for the fresh catalyst, indicate the existence of
503 different compounds from the reaction mixture, which were adsorbed on the catalyst surface.

504 **5. Conclusion**

505 The pilot plant with the capacity of 100 liters of biodiesel per day was successfully
506 designed and tested for biodiesel production from soybean oil catalyzed by $\text{MnCO}_3/\text{Na-silicate}$.
507 The kinetic model with the parameters determined based on the analysis of the experiments
508 realized in batch autoclave at 175 °C and 25 bar over $\text{MnCO}_3/\text{Na-silicate}$ as a catalyst and taking
509 into account the influence of temperature and catalyst loading on the apparent reaction rate
510 constant, was used for the design of PBTR as a main equipment of corresponding pilot plant.

511 Test of continuous operation was used to prove designed capacity and operational
512 characteristics of pilot plant unit. Investigation was started using PBTR filled only with glass
513 beads for 11 h, and then, the catalyzed transesterification of soybean oil with $\text{MnCO}_3/\text{Na-silicate}$
514 as catalyst was realized during 85 h of continuous operation. Two complete mass balances
515 performed for detailed examination of the content of produced biodiesel revealed high TAG
516 conversion (99.8%) and FAME yield over 97.5%, while the sample of used catalyst withdrawn
517 from reactor after 85 h of continuous process did not show any noticeable structural changes.
518 The results of the performed tests in pilot plant showed a good starting point for further
519 experiments planned to be done in order to improve constructed biodiesel production facility and
520 to test other types of catalysts.

521 **Acknowledgements**

522 This study was supported by the International S&T Cooperation Program of China (Grant
523 No. 2013DFG92250) as well as the research Grant No. 45001 of the Ministry of Education,
524 Science and Technological Development of the Republic of Serbia.

525 **References**

526 [1] Kouzu M, Hidaka J, Komichi Y, Nakano H, Yamamoto M. A process to transesterify
527 vegetable oil with methanol in the presence of quick lime bit functioning as solid base
528 catalyst. *Fuel* 2009;88:1983–90. doi:10.1016/j.fuel.2009.03.013.

- 529 [2] Miladinović MR, Krstić JB, Tasić MB, Stamenković OS, Veljković VB. A kinetic study
530 of quicklime-catalyzed sunflower oil methanolysis. *Chem Eng Res Des* 2014;92:1740–52.
531 doi:10.1016/j.cherd.2013.11.023.
- 532 [3] Reyero I, Arzamendi G, Gandía LM. Heterogenization of the biodiesel synthesis catalysis:
533 CaO and novel calcium compounds as transesterification catalysts. *Chem Eng Res Des*
534 2014;92:1519–30. doi:10.1016/j.cherd.2013.11.017.
- 535 [4] Roschat W, Phewphong S, Thangthong A, Moonsin P, Yoosuk B, Kaewpuang T, et al.
536 Catalytic performance enhancement of CaO by hydration-dehydration process for
537 biodiesel production at room temperature. *Energ Convers Manag* 2018;165:1–7.
538 doi:10.1016/j.enconman.2018.03.047.
- 539 [5] Jookjantra K, Wongwuttanasatian T. Optimisation of biodiesel production from refined
540 palm oil with heterogeneous CaO catalyst using pulse ultrasonic waves under a vacuum
541 condition. *Energ Convers Manag* 2017;154:1–10. doi:10.1016/j.enconman.2017.10.050.
- 542 [6] Kesic Z, Lukic I, Zdujic M, Mojovic L, Skala D. Calcium oxide based catalysts for
543 biodiesel production: A review. *Chem Ind Chem Eng Q* 2016;22:391–408.
544 doi:10.2298/CICEQ160203010K.
- 545 [7] Guo F, Wei NN, Xiu ZL, Fang Z. Transesterification mechanism of soybean oil to
546 biodiesel catalyzed by calcined sodium silicate. *Fuel* 2012;93:468–72.
547 doi:10.1016/j.fuel.2011.08.064.
- 548 [8] Wan L, Liu H, Nasreen S, Lukic I, Skala D. High temperature transesterification of
549 soybean oil with methanol using manganese carbonate as catalyst. *Chem Ind Chem Eng Q*
550 2018;124:9–22. doi:10.2298/CICEQ170221013W.
- 551 [9] Zhang Y, Liu H, Zhu X, Lukic I, Zdujic M, Shen X, et al. Biodiesel synthesis and kinetic
552 analysis based on $MnCO_3/Na$ silicate as heterogeneous catalyst. *J Serb Chem Soc*
553 2018;83:345–65. doi:10.2298/JSC170612005Z.
- 554 [10] Yang X-X, Wang Y-T, Yang Y-T, Feng E-Z, Luo J, Zhang F, et al. Catalytic
555 transesterification to biodiesel at room temperature over several solid bases. *Energ*
556 *Convers Manag* 2018;164:112–21. doi:10.1016/j.enconman.2018.02.085.
- 557 [11] Feng Y, Zhang A, Li J, He B. A continuous process for biodiesel production in a fixed bed

- 558 reactor packed with cation-exchange resin as heterogeneous catalyst. *Bioresour Technol*
559 2011;102:3607–9. doi:10.1016/j.biortech.2010.10.115.
- 560 [12] Ren Y, He B, Yan F, Wang H, Cheng Y, Lin L, et al. Continuous biodiesel production in a
561 fixed bed reactor packed with anion-exchange resin as heterogeneous catalyst. *Bioresour*
562 *Technol* 2012;113:19–22. doi:10.1016/j.biortech.2011.10.103.
- 563 [13] Xiao Y, Gao L, Xiao G, Fu B, Niu L. Experimental and modeling study of continuous
564 catalytic transesterification to biodiesel in a bench-scale fixed-bed reactor. *Ind Eng Chem*
565 *Res* 2012;51:11860–5. doi:10.1021/ie202312z.
- 566 [14] Lukić I, Kesić Ž, Maksimović S, Zdujić M, Liu H, Krstić J, et al. Kinetics of sunflower
567 and used vegetable oil methanolysis catalyzed by CaO·ZnO. *Fuel* 2013;113:367–78.
568 doi:10.1016/j.fuel.2013.05.093.
- 569 [15] Stamenković OS, Veljković VB, Todorović ZB, Lazić ML, Banković-Ilić IB, Skala DU.
570 Modeling the kinetics of calcium hydroxide catalyzed methanolysis of sunflower oil.
571 *Bioresour Technol* 2010;101:4423–30. doi:10.1016/j.biortech.2010.01.109.
- 572 [16] Veljković VB, Stamenković OS, Todorović ZB, Lazić ML, Skala DU. Kinetics of
573 sunflower oil methanolysis catalyzed by calcium oxide. *Fuel* 2009;88:1554–62.
574 doi:10.1016/j.fuel.2009.02.013.
- 575 [17] Chantrasa A, Phlernjai N, Goodwin JG. Kinetics of hydrotalcite catalyzed
576 transesterification of tricaprylin and methanol for biodiesel synthesis. *Chem Eng J*
577 2011;168:333–40. doi:10.1016/j.cej.2011.01.033.
- 578 [18] Dossin TF, Reyniers MF, Marin GB. Kinetics of heterogeneously MgO-catalyzed
579 transesterification. *Appl Catal B Environ* 2006;62:35–45.
580 doi:10.1016/j.apcatb.2005.04.005.
- 581 [19] Ilgen O, Akin AN. Determination of reaction orders for the transesterification of canola
582 oil with methanol by using KOH/MgO as a heterogeneous catalyst. *Appl Catal B Environ*
583 2012;126:342–6. doi:10.1016/j.apcatb.2012.07.034.
- 584 [20] Xiao Y, Gao L, Xiao G, Lv J. Kinetics of the transesterification reaction catalyzed by
585 solid base in a fixed-bed reactor. *Energ Fuel* 2010;24:5829–33. doi:10.1021/ef100966t.
- 586 [21] Hsieh LS, Kumar U, Wu JCS. Continuous production of biodiesel in a packed-bed reactor

587 using shell-core structural $\text{Ca}(\text{C}_3\text{H}_7\text{O}_3)_2/\text{CaCO}_3$ catalyst. Chem Eng J 2010;158:250–6.
588 doi:10.1016/j.cej.2010.01.025.

589 [22] Kapil A, Wilson K, Lee AF, Sadhukhan J. Kinetic Modeling studies of heterogeneously
590 catalyzed biodiesel synthesis reactions. Ind Eng Chem Res 2011;110107112719009.
591 doi:10.1021/ie101403f.

592 [23] Miladinovic M, Tasic M, Stamenkovic O, Veljkovic V, Skala D. Further study on kinetic
593 modeling of sunflower oil methanolysis catalyzed by calcium-based catalysts. Chem Ind
594 Chem Eng Q 2016;22:137–44. doi:10.2298/CICEQ150618027M.

595 [24] Tasić MB, Miladinović MR, Stamenković OS, Veljković VB, Skala DU. Kinetic
596 modeling of sunflower oil methanolysis catalyzed by calcium-based catalysts. Chem Eng
597 Technol 2015;38:1550–6. doi:10.1002/ceat.201500076.

598 [25] Liu Y, Wang L. Biodiesel production from rapeseed deodorizer distillate in a packed
599 column reactor. Chem Eng Process Process Intensif 2009;48:1152–6.
600 doi:10.1016/j.cep.2009.04.001.

601 [26] Marinković DM, Miladinović MR, Avramović JM, Krstić IB, Stanković M V.,
602 Stamenković OS, et al. Kinetic modeling and optimization of sunflower oil methanolysis
603 catalyzed by spherically-shaped $\text{CaO}/\gamma\text{-Al}_2\text{O}_3$ catalyst. Energ Convers Manag
604 2018;163:122–33. doi:10.1016/j.enconman.2018.02.048.

605 [27] Miladinović MR, Stamenković OS, Veljković VB, Skala DU. Continuous sunflower oil
606 methanolysis over quicklime in a packed-bed tubular reactor. Fuel 2015;154:301–7.
607 doi:10.1016/j.fuel.2015.03.057.

608 [28] Miladinović MR, Stamenković OS, Banković PT, Milutinović-Nikolić AD, Jovanović
609 DM, Veljković VB. Modeling and optimization of sunflower oil methanolysis over
610 quicklime bits in a packed bed tubular reactor using the response surface methodology.
611 Energ Convers Manag 2016;130:25–33. doi:10.1016/j.enconman.2016.10.020.

612 [29] Bournay L, Casanave D, Delfort B, Hillion G, Chodorge JA. New heterogeneous process
613 for biodiesel production: A way to improve the quality and the value of the crude glycerin
614 produced by biodiesel plants. Catal Today 2005;106:190–2.
615 doi:10.1016/j.cattod.2005.07.181.

- 616 [30] McNeff C V., McNeff LC, Yan B, Nowlan DT, Rasmussen M, Gyberg AE, et al. A
617 continuous catalytic system for biodiesel production. *Appl Catal A Gen* 2008;343:39–48.
618 doi:10.1016/j.apcata.2008.03.019.
- 619 [31] Melero JA, Bautista LF, Iglesias J, Morales G, Sánchez-Vazquez R. Production of
620 biodiesel from waste cooking oil in a continuous packed bed reactor with an agglomerated
621 Zr-SBA-15/bentonite catalyst. *Appl Catal B Environ* 2014;145:197–204.
622 doi:10.1016/j.apcatb.2013.02.050.
- 623 [32] Allain F, Portha J-F, Girot E, Falk L, Dandeu A, Coupard V. Estimation of kinetic
624 parameters and diffusion coefficients for the transesterification of triolein with methanol
625 on a solid $ZnAl_2O_4$ catalyst. *Chem Eng J* 2016;283:833–45.
626 doi:10.1016/j.cej.2015.07.075.
- 627 [33] Lin HC, Tan CS. Continuous transesterification of coconut oil with pressurized methanol
628 in the presence of a heterogeneous catalyst. *J Taiwan Inst Chem Eng* 2014;45:495–503.
629 doi:10.1016/j.jtice.2013.06.015.
- 630 [34] Tran D-T, Chang J-S, Lee D-J. Recent insights into continuous-flow biodiesel production
631 via catalytic and non-catalytic transesterification processes. *Appl Energy* 2017;185:376–
632 409. doi:10.1016/j.apenergy.2016.11.006.
- 633 [35] Kouzu M, Fujimori A, Suzuki T, Koshi K, Moriyasu H. Industrial feasibility of powdery
634 CaO catalyst for production of biodiesel. *Fuel Process Technol* 2017;165:94–101.
635 doi:10.1016/j.fuproc.2017.05.014.
- 636 [36] Glisic SB, Orlović AM. Review of biodiesel synthesis from waste oil under elevated
637 pressure and temperature: Phase equilibrium, reaction kinetics, process design and techno-
638 economic study. *Renew Sustain Energy Rev* 2014;31:708–25.
639 doi:10.1016/j.rser.2013.12.003.
- 640 [37] Nasreen S, Liu H, Lukic I, Qurashi L, Skala D. Heterogeneous kinetics of vegetable oil
641 transesterification at high temperature. *Chem Ind Chem Eng Q* 2016;22:419–29.
642 doi:10.2298/CICEQ160107011N.
- 643 [38] Di Serio M, Ledda M, Cozzolino M, Minutillo G, Tesser R, Santacesaria E.
644 Transesterification of soybean oil to biodiesel by using heterogeneous basic catalysts. *Ind*

- 645 Eng Chem Res 2006;45:3009–14. doi:10.1021/ie051402o.
- 646 [39] Suppes G. Transesterification of soybean oil with zeolite and metal catalysts. Appl Catal
647 A Gen 2004;257:213–23. doi:10.1016/j.apcata.2003.07.010.
- 648 [40] Silva CCCM, Ribeiro NFP, Souza MMVM, Aranda DAG. Biodiesel production from
649 soybean oil and methanol using hydrotalcites as catalyst. Fuel Process Technol
650 2010;91:205–10. doi:10.1016/j.fuproc.2009.09.019.
- 651 [41] Lee H V, Juan JC, Binti Abdullah NF, Nizah Mf R, Taufiq-Yap YH. Heterogeneous base
652 catalysts for edible palm and non- edible Jatropha- based biodiesel production. Chem Cent
653 J 2014;8:1–9. doi:10.1186/1752-153X-8-30.
- 654 [42] Umdu ES, Tuncer M, Seker E. Transesterification of Nannochloropsis oculata microalga's
655 lipid to biodiesel on Al₂O₃ supported CaO and MgO catalysts. Bioresour Technol
656 2009;100:2828–31. doi:10.1016/j.biortech.2008.12.027.
- 657 [43] Wan L, Liu H, Skala D. Biodiesel production from soybean oil in subcritical methanol
658 using MnCO₃/ZnO as catalyst. Appl Catal B Environ 2014;152-153:352–9.
659 doi:10.1016/j.apcatb.2014.01.033.
- 660 [44] Yin JZ, Ma Z, Hu DP, Xiu ZL, Wang TH. Biodiesel production from subcritical methanol
661 transesterification of soybean oil with sodium silicate. Energ Fuel 2010;24:3179–82.
662 doi:10.1021/ef100101m.
- 663 [45] Lukić I, Krstić J, Glišić S, Jovanović D, Skala D. Biodiesel synthesis using K₂CO₃/Al-O-
664 Si aerogel catalysts. J Serb Chem Soc 2010;75:789–801. doi:10.2298/JSC090707047L.
- 665 [46] Glišić S, Lukć I, Skala D. Biodiesel synthesis at high pressure and temperature: Analysis
666 of energy consumption on industrial scale. Bioresour Technol 2009;100:6347–54.
667 doi:10.1016/j.biortech.2009.07.024.
- 668 [47] Mirghani MES, Kabbashi NA, Alam MZ, Qudsieh IY, Alkatib MFR. Rapid Method for
669 the determination of moisture content in biodiesel using FTIR spectroscopy. J Am Oil
670 Chem Soc 2011;88:1897–904. doi:10.1007/s11746-011-1866-0.

671

672

673 **Nomenclature**

674	c_{TAG}	concentration of TAG, mol/L
675	$c_{TAG,0}$	initial concentration of TAG, mol/L
676	c_w	catalyst concentration, % (<i>w</i> , mass of catalyst per 100 g of soybean oil)
677	c_p	mass heat capacity of reaction mixture, kJ/kg·K
678	c_{FAME}	concentration of FAME, mol/L
679	d	catalyst particle diameter, mm
680	DAG	diacylglycerols
681	$FAME$	fatty acid methyl esters
682	$F_{TAG,0}$	molar flow rate of TAGs, mol/min
683	$(-\Delta H_r)$	heat effect of TAG transesterification reaction, kJ/mol
684	k_{app}	apparent reaction rate constant of transesterification process, min^{-1}
685	k_{LT}	reaction rate constant valid up to 423 K, min^{-1}
686	k_{HT}	reaction rate constant valid above 423 K, min^{-1}
687	$k_{app(w)}$	apparent reaction rate constant as function of catalysts concentration, min^{-1}
688	k_{mt}	mass transfer coefficient during transesterification process, min^{-1}
689	k_{mt0}	mass transfer coefficient at the beginning of transesterification process, min^{-1}
690	m_0	mass flow rate of reaction mixture, kg/h
691	$m_{TAG,0}$	mass flow rate of TAGs into PBTR, kg/h
692	M_0	molar flow rate of reaction mixture, mol/h
693	MAG	monoacylglycerols

694 $(-r_{TAG})$ rate of triacylglycerols transesterification, mol/(min·L)

695 t time, min

696 T temperature, K

697 TAG triacylglycerols

698 V volume of reaction mixture, L

699 x_{TAG} degree of TAG conversion

700 **Greek symbols**

701 α parameter of kinetic model, Eq. (3b)

702 β parameter of kinetic model, Eq. (3b)

703 τ residence time, min

704